Density functional theory study of the structural, electronic, and magnetic properties of dilute Cr-X alloys (X=Fe, Ru–Sb, Ta)

S. Javad Hashemifar, Nahid Ghaderi, Sedighe Sirousi, and Hadi Akbarzadeh*
Department of Physics, Isfahan University of Technology, 84156 Isfahan, Iran
(Received 24 August 2005; revised manuscript received 12 December 2005; published 12 April 2006)

In this research we have used the full-potential linearized augmented plane wave method based on the density functional theory, within the generalized gradient approximation, to study Fe, Ta, and 4*d* impurities (Ru–Sb) in a chromium system. The effects of these impurities on the structural, electronic, and magnetic properties of chromium are discussed with special emphasis on the hyperfine interaction. It is shown that the filled *d* shell 4*d* atoms are nonmagnetic with weak bonding while other impurities have considerable magnetic moments and stronger coupling with the nearest neighbors. Two different magnetic states are identified for Fe impurity in the Cr host, one with high and the other with low magnetic moments, the latter being theoretically more stable, in agreement with experimental observations. Our calculated hyperfine fields on the impurities are highly overestimated, compared with the experimental results. Such overestimation can be improved by implementing a simple model based on the scaling behavior of magnetic properties in chromium. The overestimation factor obtained by this model can be used for predicting hyperfine field values on 4*d* impurities in a Cr host.

DOI: 10.1103/PhysRevB.73.165111 PACS number(s): 71.20.Be

I. INTRODUCTION

Due to their very special properties, chromium and its alloys are among the most interesting magnetic materials. In addition to their high temperature applicability, high creep, and oxidation resistance,[1] these materials exhibit a great variety of antiferromagnetic (AF) properties[2–4] which originate from the peculiar magnetic behavior of simple bcc chromium. It has an incommensurate spin density wave (ISDW) at ground state and shifts to a paramagnetic phase through a weak first order transition at a Neel temperature of 311 K (Neel transition). The magnetic properties of chromium can be greatly modified by dissolved solute atoms. For example, samples with 0.2% vanadium[5] or with 0.7% rhodium[6] exhibit second order Neel transitions, while the addition of 1.5% Mn to the chromium[2] changes its ISDW ground state to a commensurate AF state and alloying it with 3.8% vanadium[2] leads to a paramagnetic ground state. Several approaches have been proposed to explain the profound effects of impurities on the magnetic properties of chromium.[3,7,8]

It is well understood that the hyperfine field (B_{hf}) measurement can be considered as a reliable method to study the magnetic properties of Cr and its alloys.[9,10] The first convincing experiment was performed by Street and Window (1966) using the Mössbauer effect with ^{119}Sn as the probe. Later on, Venegas *et al.*, using a time-differential perturbed angular correlation technique, studied the variation of B_{hf} on the ^{111}Cd probe with temperature and demonstrated two magnetic phase transitions for chromium.[11] Recently, Dubiel *et al.* using Mössbauer spectroscopy studied the magnetic properties of the presurface zone of the bulk, single-crystal Cr(110) implanted with ^{119}Sn ions, and found a strong enhancement of the magnetic hyperfine field in the near surface zone.[12] In contrast to the well established ferromagnetic hosts, in which B_{hf} has been measured on many probes, in an ISDW antiferromagnetic chromium host, only five elements (to our knowledge) have been used so far as a probe for B_{hf} measurements.[11]

Substantial efforts on density functional theory (DFT) have shown that this approach in its standard form is probably inadequate to predict the true magnetic properties of chromium.[13–25] While the local density approximation (LDA) leads to a nonmagnetic ground state for Cr, the generalized gradient approximation (GGA) predicts a commensurate AF state with a highly overestimated magnetic moment that is slightly more stable than the actual ISDW ground state.[25] Recently, attempts have been made to develop a new form of DFT capable of studying SDW systems such as chromium.[26] We could not find any numerical study in the literature about the hyperfine interaction in a Cr host.

In this paper we use DFT to study the hyperfine interactions on dilute impurities in a Cr host. The selected impurities were some of the 4*d* elements (Ru–Sb) as well as Fe and Ta probes. The last two probes were added to our calculations as their experimental results were available. In Sec. II the technical details of our calculations are explained. Results and discussions are presented in Secs. III and IV. In Sec. III, the structural and electronic effects of impurities on chromium are investigated. The magnetic properties and hyperfine interactions in dilute alloys are discussed in Sec. IV. Section V of the paper summarizes the conclusions of the study.

II. METHOD

As a generally acceptable procedure we used supercells to study the impurities in the Cr host. Although the available experimental data were limited to low concentrations ($\sim$1000 ppm),[11] (to avoid huge time consumption) we confined our calculations to a supercell constructed from 8 bcc unit cells; two pure Cr unit cells in each direction. The minimum impurity concentration that can be studied within this supercell, 1/16=6.25%, is much larger than the corresponding available experimental values. However, Cottenier *et al.*,[27] in a similar calculation, have shown that due to the

locality of hyperfine interaction such a concentration is small enough for simulating dilute alloys. As the applied supercell was not large enough to accommodate the ISDW state of chromium, we had to limit our calculations to the commensurate AF state and the following arguments justify our approach.

(1) The incommensurate character of the spin density wave is highly sensitive to impurities. According to Venema *et al.*,[28] for alloys with a valence electron to atom ratio n smaller than that of pure chromium, 6, the SDW wave vector decreases by the addition of the impurity; while for alloys with n larger than 6, the wave vector increases to become commensurate with the crystal lattice for $n \geqslant 6.005$. It has been shown that the adding of 0.78% Re,[29] 1.5% Mo,[2] or 2.3% Fe[30,31] to Cr, changes the ISDW to a commensurate AF state. Additionally, the measurements of Dubiel *et al.*[9,10] have shown that at concentrations above 0.7% Sn has the same behavior as Mn (when substituted in Cr) and hence it is reasonably expected for a Cr-Sn alloy at 6.25% concentration to have a commensurate ground state. Furthermore, experimental studies[32,33] have shown that Rh impurity in chromium acts similar to Re at low concentrations ($<10\%$) and hence it is expected that $Cr_{15}Rh$ alloys will have a commensurate AF ground state too.

(2) Previous numerical efforts have confirmed that many properties of pure chromium can be extracted from its virtual paramagnetic and commensurate AF phases. As an example, the incommensurate parameter, the hard modes behavior under pressure, or even the qualitative effect of impurity on them can be studied within the nesting model in the paramagnetic phase while structural and some magnetic properties of Cr in the ground state can be determined correctly using the commensurate AF phase.

Our calculations were performed within the framework of DFT using the highly accurate all-electron full potential linearized augmented plane wave (FP-LAPW) method implemented in the WIEN2K code.[34] In this procedure, every unit cell volume is partitioned into two regions: (i) nonoverlapping muffin-tin spheres around each atom and (ii) the remaining interstitial area. Two different sets of basis functions are used in the two regions. For the wave functions inside the atomic sphere a linear combination of radial functions times spherical harmonics and in the interstitial region a plane wave expansion is used. The charge density and potential are expanded into lattice harmonics inside muffin-tin spheres and as a Fourier series in the remaining space. The maximum quantum number for atomic wave functions inside the sphere was confined to $l_{max}=10$ and the energy cutoff for plane wave expansion of wave functions in the interstitial region was chosen to be 12.8 Ryd. A muffin-tin radius of 2.1 a.u. for Cr atoms and 2.35 a.u. for the impurities had been used and a mesh of 56 k points was generated in the irreducible wedge of the Brillouin zone. For the exchange-correlation potential we used the Perdew, Burke, and Ernzerhof (PBE) formalism of the generalized gradient approximation (GGA).[35] Our calculations for the valence electrons were performed in a scalar-relativistic approximation, while the core electrons were treated fully relativistically. Since Ta is a heavy element, for alloys containing such impurity the spin-orbit interaction was included.

TABLE I. The structural properties and the spin polarization of the $Cr_{15}X$ alloys and pure Cr. Cr-expt indicates the experimental values for chromium (Ref. 2) except for the lattice parameter which is twice the measured value (to be comparable with the lattice parameter of the alloys supercell); a (a.u.): the equilibrium lattice parameter; d_{nn} (a.u.): the nearest neighbor distance to impurity; R_c (a.u.): the atomic covalent radius of impurity (Ref. 36); B (GPa): bulk modules; E_C (Ry): the cohesive energy per unit of $Cr_{15}X$; E_M (m Ry): the magnetization energy per unit of $Cr_{15}X$ is defined as the minimum energy difference of the magnetic and nonmagnetic phases. P (%): spin polarization at the Fermi level (see text).

X	a	d_{nn}	R_c	B	E_C	E_M	P
Fe_f	10.81	4.704	2.19	190	−5.11	−16	30
Fe_q	10.82	4.690	2.19	194	−5.12	−21	−2
Ru	10.89	4.778	2.36	193	−5.26	−18	−12
Rh	10.91	4.811	2.36	185	−5.18	−26	−42
Pd	10.95	4.864	2.42	163	−4.98	−30	−42
Ag	11.03	4.925	2.53	141	−4.78	−31	2
Cd	11.05	4.945	2.66	135	−4.65	−37	38
In	11.07	4.953	2.83	158	−4.81	−42	−7
Sn	11.05	4.947	2.65	163	−4.92	−32	65
Sb	11.01	4.931	2.66	167	−4.88	−17	65
Ta	10.95	4.828	2.53	185	−5.35	−5	38
Cr	10.83	4.690	2.23	189	−5.10	−15	0
Cr-expt	10.90			190	−4.82		

III. STRUCTURAL AND ELECTRONIC PROPERTIES

The cubic supercell used in our calculations consists of eight bcc chromium unit cells ($2\times2\times2$), with one of the 16 Cr atoms substituted by impurity X (Fe, Ru–Sb, Ta). The nonequivalent atoms in such supercells are classified according to X (0,0,0), Cr1 (u,u,u), Cr2 (0.5,0,0), Cr3 (0.5,0.5,0), and Cr4 (0.5,0.5,0.5). The labels of Cr atoms are consistent with their distances from impurity (larger numbers correspond to longer distances). Due to the inhomogeneous environment of Cr1 at its ideal positions ($u=0.25$), the internal parameter needs to be relaxed. In order to find the equilibrium lattice parameters, the energy of the supercell was calculated at different volumes for all impurities with full internal relaxation up to force convergence of 1 mRyd/a.u. for each volume. By fitting the calculated data with the Murnaghan equation of state, structural properties were calculated and listed in Table I along with the corresponding values for pure chromium.

The calculated values for pure chromium, except for the cohesive energy, are in reasonable agreement with the experimental results. The error in the cohesive energy may be partly attributed to the commensurate assumption of the ground state in our calculations.

We found out that for the Fe alloy, by adjusting the initial charge density, the self-consistent procedure can lead to two different results. In one case, Fe carries a rather large magnetic moment ($\sim1.8\mu_B$) antiparallel to the magnetic moment of Cr1 and so we call it the free magnetic phase. In the other case (quenched magnetic phase) the iron atom has a much

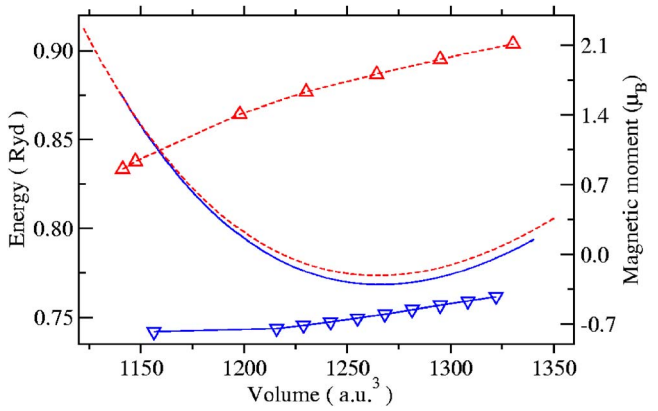

FIG. 1. (Color online) Lines: Variation of the total energy (left axis) as a function of volume for free (dashed line) and quenched (solid line) magnetic phases of Fe. Symbol-lines: Volume dependence of the Fe magnetic moments (right axis) in Fe_f (△) and Fe_q (▽) alloys.

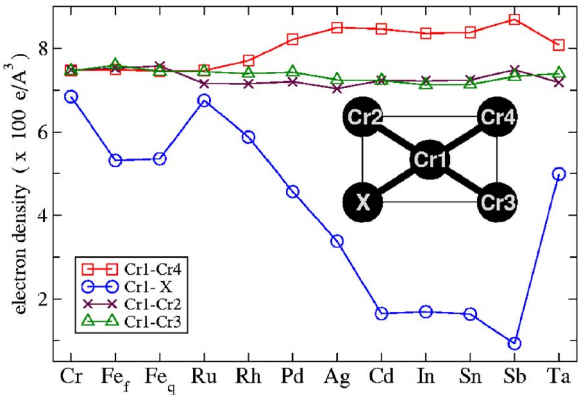

FIG. 2. (Color online) The maximum values of the difference electron density at the four nearest neighbor bonds. Inset: The four nearest neighbor bonds shown in [011] plane.

smaller magnetic moment ($\sim 0.6\mu_B$) parallel to Cr1 magnetic moment. The energy-volume curves of these two phases, compared to each other in Fig. 1, indicate more stability for the quenched phase and a transit to the free magnetic phase at a pressure of about 24 GPa. The structural properties (Table I) of these two phases are very similar while their magnetic properties are quite different. This will be discussed in the next section. Hereafter we use symbols of Fe_f and Fe_q for the free and quenched magnetic phases of $Cr_{15}Fe$ alloys, respectively.

We use the parameters in Table I to investigate the effect of dilute impurities on the structural properties of chromium. It is clearly seen that for 4*d* impurities (Ru–Sb), the bulk modules as well as the cohesive energy decrease from Ru to Cd and then increase, predicting that the Cd alloy has the weakest bond in this series. The other systematic behavior observed for the lattice parameters and d_{nn} values increase from Ru to In and then start to decrease. The nearly similar trend followed by lattice parameters, d_{nn}, and the atomic covalent radius shown in Table I, is an indication of the covalent character of the existing bonds between impurities and their nearest Cr neighbors.

For a better understanding of the bonds strength in our systems, we calculated the maximum value of difference electron densities (crystal charge density minus atomic charge density) along the nearest neighbor bonds and plotted them in Fig. 2. The four nearest neighbor bonds in the supercell are shown in the [011] plane (inset of Fig. 2). This plot can be used for a qualitative comparison of the bonds strength in the different alloys. It is clearly seen that the *X* -Cr1 bond for all alloys, except *X*=Ru, is weaker than the pure system. For the 4*d* impurities used in our calculation the bond strength decreases smoothly from Ru to Sb although it looks practically unchanged between Cd and Sn. This is generally consistent with the lattice constant, bulk modules, and cohesive energy behavior for the same impurities (Table I) and shows that Cr1-impurity coupling with 4*d* elements is the main source of different structural properties. The Cr1 -Cr4 bond strength increases slowly in the range of Ru–Ag and then remains essentially constant while the Cr1-Cr2 and Cr1-Cr3 bonds are practically not affected by the impurity.

Figure 3 shows the total and atom projected density of states of impurity and Cr1 for all alloys at their equilibrium lattice parameters. We observe that, compared to other impurities, Fe in general and Fe_q in particular have the highest degrees of hybridization with Cr1. For all alloys containing 4*d* elements, the *d* electrons are the main constituent of the valence band and by going from Ru to Sb, the DOS of the impurity are moving away from the Fermi energy. Therefore by filling the 4*d* shell, the hybridization between the impurity and Cr1 atom decreases which is in good agreement with the behavior of the *X*-Cr1 bond and the observed structural properties. In the filled 4*d* shell impurities (Cd, In, Sn, Sb) the *d* electrons are well localized below the Fermi level (not shown in the figure) and therefore the hybridization and con-

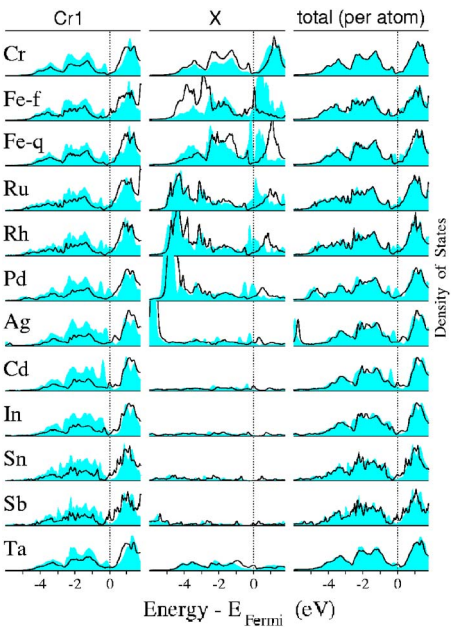

FIG. 3. (Color online) The calculated majority (solid lines) and minority (shaded areas) density of states of the alloys projected into total (per atom), impurity (*X*), and Cr1 components.

TABLE II. The atomic magnetic moments (μ_B) of alloys at their theoretical lattice constants. For impurities the partial magnetic moments are also listed. No impurities: magnetic moments of Cr atoms in the optimized supercell of alloys but after substituting impurity with vacancy. Pure: the magnetic moment of a Cr atom in a pure antiferromagnetic chromium with the alloy equilibrium lattice constants.

	Impurity				Cr Atoms		No Impurities		Pure
	D	D_{eg}	D_{t2g}	Total	Cr1	Cr4	Cr1	Cr4	Cr
Fe_f	1.80	0.88	0.92	1.81	−0.92	0.90	−1.06	0.85	0.99
Fe_q	−0.59	−0.90	0.31	−0.61	−1.05	1.02	−1.06	0.88	1.00
Ru	0.17	−0.11	0.28	0.16	−1.04	0.96	−1.36	1.00	1.12
Rh	−0.21	−0.36	0.15	−0.22	−1.21	0.94	−1.51	1.03	1.16
Pd	−0.25	−0.23	−0.02	−0.26	−1.36	0.86	−1.67	1.07	1.23
Ag	−0.15	−0.08	−0.07	−0.16	−1.58	1.00	−1.81	1.16	1.36
Cd	−0.05	0.00	−0.04	−0.05	−1.53	1.06	−1.84	1.17	1.41
In	−0.02	0.01	−0.03	0.00	−1.51	1.08	−1.86	1.19	1.43
Sn	−0.02	0.01	−0.03	0.00	−1.38	0.96	−1.83	1.16	1.40
Sb	−0.01	0.01	−0.02	0.00	−1.13	0.80	−1.77	1.70	1.33
Ta	0.15	0.05	0.10	0.15	−0.87	0.72	−1.63	1.11	1.22

sequently the bond strength between the Cr1 atom and the impurity is very low.

Although the coupling of the nearest neighboring Cr atoms in all of the considered compounds is antiferromagnetic, the presence of impurity atoms breaks the equivalency of the two nearest neighboring Cr atoms and leads to a ferrimagnetic state for the alloys. Therefore as is obvious in the DOS plots (Fig. 3) the spin polarizations at the Fermi level of alloys, in contrast to an ideal antiferromagnet, are not zero. The spin polarization P, which is an important parameter in magnetoelectronic studies, can be defined as $P=[N_{\uparrow}(E_F)-N_{\downarrow}(E_F)]/N(E_F)$, where N is the density of states, E_F is the Fermi energy, and the up and down arrows indicate the majority and minority spins, respectively. The obtained values of P in alloys are listed in Table I and in some cases their values are quite comparable with the spin polarizations of a ferromagnetic material.

The total DOS plots (Fig. 3) show that all systems are metals while their Fermi level locations in a pseudogap indicate some covalent feature for the bonds. By comparing the total charges located inside the atomic spheres of Cr atoms in the alloys and the pure system, we found out that there is no considerable charge transfer between the impurities and Cr atoms and for this reason the ionic character of the bonds are negligible. Hence we conclude that the mechanism of bonding in the studied compounds are mainly metallic covalent.

In addition to what has been discussed so far, exhibiting the following behavior in these alloys needs further speculation. Figure 3 shows that the Fermi level in some alloys is located on a singular point of DOS. Recently,[29,37] similar singularities observed in Mo-Re and Cr-Re alloys were associated with the so-called electronic topological transition (ETT). ETT is a drastic change in the Fermi surface topology which can be accompanied by peculiarities in the thermodynamic potential derivatives. Although such behavior has been explained within the nonmagnetic phase of alloys, it seems that even in the magnetic states, the occurrence of an ETT transition is not completely ruled out.

IV. MAGNETIC PROPERTIES AND HYPERFINE INTERACTIONS

The calculated magnetic moments of the impurities and the chromium atoms in alloys at their theoretical lattice parameter are listed in Table II. It is clearly seen that Cd, In, Sn, and Sb atoms, with filled $4d$ shells, are nonmagnetic while other impurities have magnetic characteristics, which are mainly contributed by the polarization of their d electrons. For a better understanding of the magnetic interaction mechanism inside the alloys, the magnetic moment of Cr atoms in two other hypothetical structures were also calculated. In order to construct these two structures, supercells containing different impurities were initially optimized and then the impurities were removed from the first structure (No impurities) while they were replaced by chromium atoms in the second structure (Pure). The results obtained for these two structures (listed in Table II) can be further used to study the effects of impurities and supercell volume on the magnetic properties of alloys.

In all alloys, except Fe_q, the magnetic moments of Cr atoms increase by removing impurities and the most increment occurs for Ta alloy. In addition, the magnetic moment of a Cr1 atom in a Ta alloy (and to a smaller extent in a Sb alloy), compared to the others, is much lower than the corresponding value in the pure system. We conclude that the Ta impurity has a high diminishing effect on Cr magnetism and substantially reduces the magnetic stability of the system, which is in agreement with the lowest value of magnetization energy observed in the Ta alloy (Table I). This behavior of Ta may be attributed to the more itinerant character of $5d$ valence electrons in Ta compared to the $4d$ and $3d$ valence electrons in other impurities. The greater values of the magnetization energy for all alloys (except Ta) compared to the pure system show that enhancement of the Cr magnetic moments by substituting the impurity with vacancy in these systems is not due to any diminishing effects of these impurities but is the result of the lower coordination number of Cr1 after removing the impurity. The rather close agreement

of the Cr1 magnetic moment in these alloys with the corresponding values in pure Cr indicate that these impurities do not change the magnetic stability of the Cr host substantially and therefore we attribute the scattered values of E_M in these cases mainly to the different volumes of these systems.

As was mentioned in the previous section, we obtained two different phases for Fe alloy; namely Fe_f and Fe_q with rather identical Cr magnetic moments (Table II). The calculated cohesive and magnetic energies show that the quenched phase is the stable phase which is consistent with the experimental observations. A microscopic measurement of the hyperfine field at Fe sites by the Mössbauer effect yields a small Fe magnetic moment of approximately $0.5\mu_B$,[38–40] close to our results for Fe_q phase, while the temperature dependence of the magnetic susceptibility indicates large local moments on Fe ions in the Cr matrix,[3] which is consistent with the Fe_f phase. Shiga and Nakumara[41,42] found out that at Fe concentrations of about 6–20 %, two phases, with different Fe magnetic moments, can be observed in the Cr-Fe alloy and that around 6% of the Fe concentration (similar to our $Cr_{15}Fe$ alloy) the phase with the low Fe magnetic moment is the most probable phase, which is in agreement with the lower magnetic energy of the quenched phase. By comparing Fe magnetic moments at different volumes (Fig. 1), it is concluded that this property increases by increasing the volume in the free magnetic phase of the Fe alloy and decreases for the quenched system. Therefore, by choosing very large volumes (evaporating of crystal), the Fe moment in Fe_f reaches its isolated atomic value while in the Fe_q phase it vanishes. We therefore conclude that in the Fe_q alloy the inherent magnetic character of Fe is completely quenched and its magnetic moments are totally due to the electronic hybridization with Cr neighbors, which is in good agreement with the observed high hybridization in the Fe_q alloy (Fig. 3).

Looking at Table II, we observe that substituting impurity with vacancy in an Fe_q alloy has almost no effect on the magnetic moment of the Cr1 atom. Hence it seems that Fe and Cr1 atoms are magnetically decoupled in this system, in agreement with what Booth observed in 1966.[43] In addition, in contrast to other alloys, the magnetic moment of Cr4 after removing impurity changes more than Cr1, although Cr1 is the nearest neighbor of the impurity. Such behavior along with the magnetic decoupling of Fe-Cr1 in the Fe_q alloy can be considered as an indication of the importance of longer (than the nearest neighbor) range magnetic interactions between Fe and Cr atoms in this phase.

A comparison between the magnetic moments of Cr4 as the furthest atom to the impurity with the corresponding value in the pure system (Table II) shows that, except for the Fe alloys, the two values are not compatible. Such inconsistency does not seem to be a long range interactional effect but is mainly due to the relaxation of the Cr1 atom, a phenomenon that is very weak in Fe alloys. In every supercell, the impurity pushes away the Cr1 from its ideal position toward the Cr4 that has eight Cr1 nearest neighbor and this relocation effectively quenches and decreases the magnetic moment of the Cr4 atom. We found that by moving back the Cr1 to its ideal position, the magnetic moment of the Cr4 returns back to its corresponding bulk value too.

TABLE III. Various components of the hyperfine field (kG) on the impurities at theoretical lattice constants. As we found that Fe_q is the stable phase of Fe alloy, the measured B_{hf} value on Fe probe is assigned to this phase.

	Core	Valence	Total	Modified	Exp.[11]
Fe_f	−219.0	154.2	−64.8	−166.7	
Fe_q	70.2	1.4	71.6	70.7	36
Ru	−8.2	36.3	28.1	4.1	
Rh	53.8	35.6	89.4	65.9	65
Pd	60.4	36.0	96.4	72.6	
Ag	33.2	93.0	126.2	64.8	
Cd	8.0	149.2	157.2	58.6	60
In	2.7	248.2	251.0	86.9	
Sn	1.6	269.8	271.4	93.1	93
Sb	1.3	229.2	230.5	79.0	
Ta	3.2	38.9	42.1	16.4	14

Now let us focus on the hyperfine interaction in dilute Cr alloys. The hyperfine field generally consists of dipolar, orbital, and Fermi contact contributions, while in the cubic symmetry, Fermi contact is the dominant term. In the Pauli approximation and within the scalar relativistic limit this term can be calculated by using the spin density of s electrons at the nuclear position $[n^s(0)]$,

$$B_{hf} = \frac{8\pi}{3}\mu_B[n^s_\uparrow(0) - n^s_\downarrow(0)].$$

To take into account the full relativistic corrections, the spin density has to be averaged over the Thomson radius.[44] Following this scheme, we calculated B_{hf} on Fe, Ta, and $4d$ impurities in the Cr host at their equilibrium lattice constants. The obtained B_{hf} values given in Table III are broken down into total, core (B^c_{hf}), and valence (B^v_{hf}) contributions.

The calculated data show a consistent trend between B^c_{hf} (Table III) and the polarization of the d valence orbital of impurities (Table II). Such results confirm that the core polarization is mainly due to the exchange interaction of the polarized d shell with the s orbitals of the core. Following the explanation of Freeman and Watson[45] this s-d exchange interaction in general is expected to be negative leading to the opposite direction of B^c_{hf} and magnetization of d electrons. This expectation is fulfilled by all of the investigated alloys except the Ta compound that has a positive s-d exchange interaction. The valence component of B_{hf} is originated from the coupling of the impurity and the neighboring Cr atoms and so it is called the *transferred* hyperfine. Since the hyperfine interaction is a local effect, B^v_{hf} is mainly determined by X-Cr1 coupling. The almost zero value of B^v_{hf} in an Fe_q alloy is another indication of the magnetic decoupling of Fe and Cr1 in this system.

A comparison between the theoretical and experimental results (Table III) shows that our DFT calculations highly overestimate the B_{hf} values in the Cr host. To make sure that this discrepancy is not due to the much higher impurity concentration used in our calculation compared to the available

experimental conditions, we repeated our calculations using a bigger supercell (a $3\times3\times3$ supercell containing 27 atoms having 1/27 impurity concentration) and found almost similar values. Additionally, in a similar work[27] it was shown that B_{hf} is not substantially sensitive to the supercell size. We then attribute this overestimation to the GGA function of the exchange correlation used in our calculations. It is accepted that GGA overestimates magnetic moments of the Cr atoms in the antiferromagnetic phase with respect to the measured values.[25] On the other hand, the LDA is not able to stabilize the antiferromagnetic ground state of Cr, although the obtained magnetic moments at the experimental lattice constants are in good agreement with the experiments. We applied the LDA to the alloys and found out a nonmagnetic ground state for all the impurities. Furthermore, at the experimental lattice constants of Cr, in one case (Cd alloy), the LDA improves the B_{hf} values but in the other it leads to a nonmagnetic or a weak magnetic state. We therefore believe that LDA is not an appropriate functional for the systematic study of the hyperfine interaction (and other magnetic properties) in Cr alloys. In the rest of the paper we try to develop a simple model for extracting a reasonable B_{hf} within the GGA.

Recently Cottenier *et al.*[24] proposed a scheme called laboratory chromium to study the magnetic properties of Cr. This model is based on the scaling behavior of the magnetic properties of the system versus the magnetic moments of Cr atoms and uses the central criteria that if one uses a lattice parameter that leads to the measured magnetic moments, the other magnetic properties of the system will also be obtained in reasonable agreement with the experiments. Such lattice constants that can essentially differ both from experimental and theoretical values are called a magic lattice constants (a_{mag}). Cottenier *et al.* suggested a value of $a_{mag}=2.81$ Å for the ISDW state of pure Cr within the GGA. In order to check the applicability of such a model in our system, We initially looked for the magic lattice constants that give the measured B_{hf} values. We found that there is not any correlation among the atomic magnetic moments in various alloys to be used as a criterion for the exact definition of the magic lattice constants for different Cr alloys. Therefore it seems that a_{mag} in these systems is a case-sensitive parameter and hence this scheme is not applicable to the systematic study of the magnetic properties of Cr alloys.

Now we implement the basic idea behind this model, the scaling behavior of magnetic properties versus magnetic moments, to develop a simple model for extracting reasonable B_{hf} from the theoretical results. As mentioned earlier, the GGA overestimates the magnetic moments of chromium and since B_{hf}^{v} originates mainly from the hybridization of impurity with the neighboring Cr atoms and is roughly proportional to the magnetic moment of nearest neighboring Cr atoms,[44] it is quite normal for the valence component of B_{hf} to be overestimated. If B_{hf}^{v} is overestimated by a factor of w, we can define a modified hyperfine field (B_{hf}^{m}) as follows:

$$B_{hf}^{m}=B_{hf}^{c}+\frac{1}{w}B_{hf}^{v}. \tag{1}$$

We found that the best fit to the experimental data could be obtained by using $w\approx2.95$. The calculated B_{hf}^{m} modified by this correction factor are listed in Table III and surprisingly, except for the Fe alloy, are in good agreement with the experimental values. In the Fe_q alloy, due to the magnetic decoupling of the impurity and Cr1 atoms, the valence component of B_{hf} is negligible and one should look for other sources of overestimation. We will discuss this at the end of this section.

More precise investigation shows that such an overestimation factor is not meaningless and can be predicted by comparing the experimental and calculated Cr magnetic moments. The effective measured value of Cr magnetic moments in the ISDW state is $0.44\mu_B$,[46] while from a numerical point of view the atomic magnetic moment is not a well defined quantity and depends on the definition of atomic spheres (muffin-tin radius). A reasonable procedure is to select these atomic spheres as big as possible, with a muffin-tin radii equal to half of the nearest neighbor distance. On the other hand, increasing the muffin-tin radius decreases the accuracy of the LAPW method. To overcome this obstacle we initially used a muffin-tin radii of 2.0 a.u. for self-consistent calculations and after obtaining the converged electron densities, the biggest possible atomic sphere was used for the calculation of Cr magnetic moments. In this way and by using DFT-GGA calculations, we finally obtained a value of $1.28\mu_B$ for Cr magnetic moments at experimental lattice constants (2.884 Å) within the commensurate antiferromagnetic state. Therefore the overestimation factor of magnetic moments with respect to the measured value is $1.28/0.44\approx2.91$, very close to the obtained overestimation factor for B_{hf}^{v}. Hence, we conclude that the origin of the overestimation of hyperfine filed in Cr alloys is probably the overestimation of magnetic moments in pure chromium.

For the Fe_q alloy the case is quite different and due to the magnetic decoupling of Fe and Cr1 such an argument does not hold. In order to find out why B_{hf} in this system is overestimated while its valence component is negligible one should consider the electronic interactions in this system. As a matter of fact, in contrast to very weak Fe-Cr1 magnetic coupling in the Fe_q alloy, it has the strongest Fe-Cr1 hybridization among the studied alloys (Fig. 3). Therefore it seems that the small magnetic moment of Fe in the quenched phase is induced by the hybridization with Cr1 and the magnetic character of Fe in this case is completely quenched. Hence the observed overestimation in Cr magnetic moments would be transfered to the Fe local moments and accordingly the core components of B_{hf} in this system is overestimated.

Let us now discuss the applicability range of this simple model and the validity of Eq. (1). In general, one expects that the overestimation of the Cr magnetic moments within the GGA leads to a similar overestimation in the local moments of impurities and hence the general form of Eq. (1) should be written as $B_{hf}^{m}=\frac{1}{w1}B_{hf}^{c}+\frac{1}{w2}B_{hf}^{v}$; both B_{hf}^{c} and B_{hf}^{v} components are rescaled but with different weights. For those impurities where B_{hf}^{v} is the dominant contribution of B_{hf}, the rescaling of B_{hf}^{c} does not have any considerable effect and Eq. (1) is well applicable to them. Therefore the calculated B_{hf}^{m} values for Cd, In, Sn, Sb, Ta, and even Ru (Table III) would be considered as reliable theoretical predictions. For those cases in which the core contribution is relatively significant, it is not clear to what extent this component has been overesti-

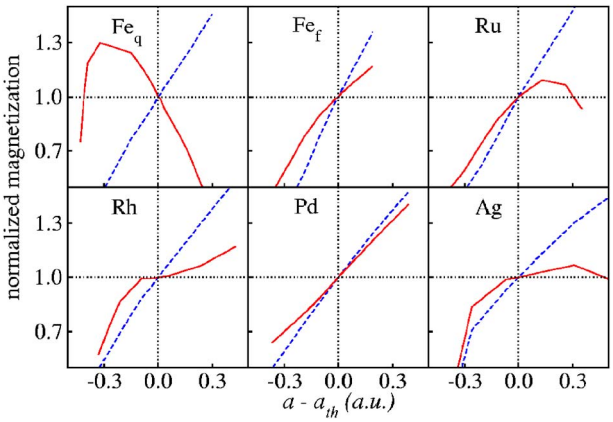

FIG. 4. (Color online) Variation of the normalized magnetic moments (magnetic moments divided by the corresponding value at the theoretical lattice parameter) of impurity (solid line) and Cr1 (dashed line) versus lattice constants a (a_{th} are the theoretical lattice constants).

mated. For example, the results for the Rh alloy show that rescaling of B_{hf}^{v} is good enough for the reproduction of a measured value and most likely B_{hf}^{c} is not overestimated while in the case of the Fe$_q$ alloy there is a high overestimation in the core component. Hence, for these systems a unique rescaling factor could not be defined for B_{hf}^{c}.

We found that by considering the volume dependence of the impurity magnetic moments one can qualitatively investigate the overestimation factor ($w1$) induced by Cr magnetic moments in the B_{hf}^{c}. Figure 4 compares the impurities and Cr1 magnetic moments (normalized to their value at theoretical lattice parameter) as a function of lattice constants for alloys with a large B_{hf}^{c} component. While Cr1 moments in all alloys around the theoretical lattice constants change rather monotonously, impurity moments in some cases do not follow such a trend. In Pd and two Fe alloys, magnetic moments of impurity and Cr1 change almost with the same absolute slope and hence it seems that impurity moments are highly influenced by Cr1 moments. As the calculated Cr moment is much higher than its real corresponding value one expects the magnetic moment of the impurity in such systems to be substantially overestimated. B_{hf}^{c} for Fe$_q$ alloys can be considered as a prototype of such systems. As the core component of B_{hf} in Fe$_q$ is probably overestimated by a factor of about 2 (Table III), by applying the same factor in the Pd alloy it is expected that the real value of the hyperfine field on such impurity (after rescaling both core and valence) to is around 42 kG. On the other hand, we observe that in Rh, Ag, and even in Ru alloys the behavior of the two curves is quite different and it seems that the impurity magnetic moments around the theoretical lattice constants are not strongly affected by the Cr1 moment. Therefore one reasonably expects that the impurity magnetic moments are not substantially overestimated in these alloys. As we see in the Rh alloy the experimental value is reproduced only by rescaling the valence component of B_{hf}. Hence for the Ag alloy we expect our predicted value for B_{hf}^{m} in Table III to be close to the real hyperfine field.

V. CONCLUSION

Using the density functional approach we have investigated the structural, electronic, and magnetic properties, as well as the hyperfine interactions in $Cr_{15}X$ alloys (X=Fe, Ru–Sb, Ta). Our results show that there are two possible magnetic states for the Fe impurity in the Cr host and the stable state is the one with a rather low Fe magnetic moment, in agreement with the experiments. We observed a rather high overestimation in the calculated hyperfine fields and attributed them to the generalized gradient approximation used in our calculations. We presented a simple model based on the rescaling of the valence component of B_{hf} using the overestimation factor obtained in the pure antiferromagnetic Cr system. The results show that this model is well applicable to the impurities that have a dominant valence contribution to the hyperfine field. It was also shown that for dilute alloys with considerable core contribution to the B_{hf}, normalized magnetic moments of impurity and its nearest Cr neighbors could be used to roughly estimate the overestimation of B_{hf}^{c}.

ACKNOWLEDGMENTS

This work was partly supported by Isfahan University of Technology. We wish to thank Stefaan Cottenier from Instituut voor Kern- en Stralingsfysica, KULeuven, Celestijnenlaan 200 D, B-3001 Leuven, Belgium for helpful discussions.

*Electronic address: akbarzad@cc.iut.ac.ir

[1] W. D. Klopp, Nasa Technical Report No. 70N20869 1970 (unpublished).
[2] E. Fawcett, Rev. Mod. Phys. **60**, 209 (1988).
[3] E. Fawcett, H. L. Alberts, V. Y. Galkin, D. R. Noakes, and J. V. Yakhmi, Rev. Mod. Phys. **66**, 25 (1994).
[4] H. Zabel, J. Phys.: Condens. Matter **11**, 9303 (1999).
[5] D. R. Noakes, T. M. Holden, and E. Fawcett, J. Appl. Phys. **67**, 5262 (1990).
[6] B. Lebech and K. Mikke, J. Phys. Chem. Solids **33**, 1651 (1972).
[7] K. Machida and M. Fujita, Phys. Rev. B **30**, 5284 (1984).
[8] A. N. Tahvildar-Zadeh, J. K. Freericks, and M. Jarrell, Phys. Rev. B **55**, 942 (1997).
[9] S. M. Dubiel, J. Magn. Magn. Mater. **124**, 31 (1993).
[10] S. M. Dubiel and J. Cielak, J. Magn. Magn. Mater. **148**, L384 (1995).
[11] R. Venegas, P. Peretto, G. N. Rao, and L. Trabut, Phys. Rev. B **21**, 3851 (1980).
[12] S. M. Dubiel, J. Cielak, J. Zukrowski, and H. Reuther, Phys. Rev. B **63**, 060406(R) (2001).
[13] T. L. Loucks, Phys. Rev. **139**, A1181 (1965).
[14] J. Rath and J. Callaway, Phys. Rev. B **8**, 5398 (1973).

[15] N. I. Kulikov, Sov. J. Low Temp. Phys. **5**, 173 (1979).
[16] N. I. Kulikov and E. T. Kulatov, J. Phys. F: Met. Phys. **12**, 2291 (1982).
[17] D. G. Laurent, J. Callaway, J. L. Fry, and N. E. Brener, Phys. Rev. B **23**, 4977 (1981).
[18] J. Kubler, *Theory of Itinerant Magnetism* (Oxford University Press, Oxford, 2000).
[19] H. L. Skriver, J. Phys. F: Met. Phys. **11**, 97 (1981).
[20] D. J. Singh and J. Ashkenazi, Phys. Rev. B **46**, 11570 (1992).
[21] V. L. Moruzzi and P. M. Marcus, Phys. Rev. B **46**, 3171 (1992).
[22] K. Hirai, J. Phys. Soc. Jpn. **66**, 560 (1997).
[23] G. Bihlmayer, T. Asada, and S. Blügel, Phys. Rev. B **62**, R11937 (2000).
[24] S. Cottenier *et al.*, J. Phys.: Condens. Matter **14**, 3275 (2002).
[25] R. Hafner, D. Spisak, R. Lorenz, and J. Hafner, Phys. Rev. B **65**, 184432 (2002).
[26] K. Capelle and L. N. Oliveira, Phys. Rev. B **61**, 15228 (2000).
[27] S. Cottenier and H. Haas, Phys. Rev. B **62**, 461 (2000).
[28] W. J. Venema *et al.*, J. Phys. F: Met. Phys. **10**, 2841 (1980).
[29] N. I. Medvedeva, Y. N. Gornostyrev, and A. J. Freeman, Phys. Rev. B **67**, 134204 (2003).
[30] A. S. Arrott, S. A. Werner, and H. Kendrick, Phys. Rev. **153**, 624 (1967).
[31] Y. Ishikawa, S. Hoshino, and Y. Endo, J. Phys. Soc. Jpn. **22**, 1221 (1967).
[32] D. Dadarlat, T. Petrisor, A. Giurgiu, and I. Pop, Phys. Status Solidi B **117**, K155 (1983).
[33] J. G. Booth, Phys. Status Solidi **7**, K157 (1964).
[34] K. Schwarz and P. Blaha, Comput. Mater. Sci. **28**, 259 (2003).
[35] J. P. Perdew, K. Burke, and M. Ernzerhof, Phys. Rev. Lett. **77**, 3865 (1996).
[36] Wiley-Vch periodic table of elements. ISBN: 3-527-10109-8 (Wiley-Vch, P.O. Box 101161, D-69451 Weinheim, Germany).
[37] N. V. Skorodumova, S. I. Simak, I. A. Abrikosov, B. Johansson, and Y. K. Vekilov, Phys. Rev. B **57**, 14673 (1998).
[38] M. B. Salamon and F. J. Feigl, J. Phys. Chem. Solids **29**, 1443 (1968).
[39] I. R. Herbert, P. E. Clark, and G. V. H. Wilson, J. Phys. Chem. Solids **33**, 979 (1972).
[40] R. B. Frankel and N. A. Blume, J. Phys. Chem. Solids **34**, 1565 (1973).
[41] M. Shiga and Y. Nakamura, Phys. Status Solidi A **37**, K89 (1976).
[42] M. Shiga and Y. Nakamura, J. Phys. Soc. Jpn. **49**, 528 (1980).
[43] J. G. Booth, J. Phys. Chem. Solids **27**, 1639 (1966).
[44] S. Blügel, H. Akai, R. Zeller, and P. H. Dederichs, Phys. Rev. B **35**, 3271 (1987).
[45] A. G. Freeman and R. E. Watson, in *Magnetism*, edited by G. T. Rado and H. Suhl (Academic, New York, 1965), Vol. II A.
[46] The magnetic momets of Cr atoms in ISDW ground state have an almost sinosoidal form with amplitude of $0.62\mu_B$. Therefore the effective magnetic moments of Cr atoms could be defined as the root mean square (rms) of magnetic moments. Supposing the sinosoidal form of variation, the rms of magnetic moment is $0.62/\sqrt{2} \simeq 0.44\mu_B$.